

DPF2015-454
September 29, 2015

Electroweak Results from the ATLAS and CMS Experiments

JUNJIE ZHU¹

*Department of Physics, University of Michigan
Ann Arbor, MI, 48109, USA*

I summarize an extensive ATLAS and CMS electroweak physics program that involves a variety of single boson, diboson, triboson, and vector boson scattering measurements. The relevance of these studies to our understanding of the electroweak sector and electroweak symmetry breaking is emphasized. I describe the recent results and prospects for future measurements.

PRESENTED AT

DPF 2015

The Meeting of the American Physical Society
Division of Particles and Fields
Ann Arbor, Michigan, August 4–8, 2015

¹Work supported by the United States Department of Energy Early Career Grant under contract de-sc0008062.

1 Introduction

Except the gluons, all fundamental particles we know experience electroweak interactions. Due to gauge symmetry and chiral symmetry, all particles are required to be massless in the Standard Model (SM) theory. SM explains the origin of mass by introducing a scalar Higgs field (ϕ) with a Mexican-hat potential: $V(\phi) = \mu^2\phi^2 + \lambda\phi^4$ with $\mu^2 < 0$ [1]. The minima of the potential happen for non-zero vacuum expectation values and break the electroweak symmetry. Massless Goldstone bosons generated from the symmetry breaking are absorbed by massless gauge bosons to become their longitudinal components of the now-massive W and Z bosons. Fermions gain their masses via Yukawa couplings with the Higgs field. The quantum excitation of the Higgs field is the Higgs boson.

Besides the neutral current and charged current interactions, gauge bosons also have self-interactions due to the non-Abelian structure of the $SU(2)_L \times U(1)_Y$ gauge symmetry group in the electroweak sector of the SM [2]. The allowed triple gauge coupling (TGC) vertices are $WW\gamma$ and WWZ , and the allowed quartic gauge coupling (QGC) vertices are $WWWW$, $WWZZ$, $WWZ\gamma$ and $WW\gamma\gamma$. The Higgs boson couples to all massive gauge bosons and fermions, it also couples to itself that results in HHH and $HHHH$ coupling vertices.

2 Global Electroweak fits and SM consistency tests

The electroweak theory is an extremely successful theory with only a few free parameters: g , g , μ and λ , where g and g are the weak and electromagnetic couplings, μ and λ are the two parameters for the Higgs potential. Other parameters like fermion masses and strong coupling constant enter by radiative corrections. With these parameters known, we can make predictions for all other quantities in the electroweak sector. In reality we often choose a few quantities measured with high precision to determine these parameters and then make predictions for other variables. We have successfully predicted the preferred top and Higgs mass ranges before the actual discoveries. With many experimental measurements performed so far, we can check the consistency of the electroweak theory and search for new physics beyond the SM.

The most recent global electroweak fits was performed by the Gfitter collaboration [3]. Six measured quantities (M_Z , M_H , α , m_t , m_b and m_c) are used as inputs. For theoretical predictions, calculations detailed in [4] and references therein are used. The predictions are compared to experimental results from low energy experiments, LEP/SLD, Tevatron and LHC [5]. Figure 1 shows comparison of the global fit results with the indirect determination in units of the total uncertainty, defined as the uncertainty of the direct measurement and that of the indirect determination added in quadrature. The indirect determination of an observable corresponds to a fit without

using the corresponding direct constraint from the measurement. The overall χ^2/dof is 17.8/14, corresponding to a probability of 21%. There are no individual deviations that exceed 3σ , showing good consistency between all measurements and theoretical predictions.

The LHC experiments provided the first direct measurement of the Higgs boson mass (m_H) [6] which is a critical input to the global fits. The uncertainties on the indirect measurement of m_W (W boson mass), $\sin^2 \theta_{eff}^\ell$ (lepton effective weak mixing angle), m_t and m_H have reduced significantly after the inclusion of the direct m_H measurement in the global fits. The fitted m_W has an uncertainty of 8 MeV while the measured value has an uncertainty of 15 MeV. The fitted $\sin^2 \theta_{eff}^\ell$ has an uncertainty of 7×10^{-5} , while the measured uncertainty is 17×10^{-5} [3]. It is thus important to further improve these two measurements.

3 $\sin^2 \theta_{eff}^\ell$ and m_W measurements

For the $q\bar{q} \rightarrow X \rightarrow \ell^+\ell^-$ process, we can have the exchange of either a photon or a Z boson. The couplings of the photon to fermions are pure vector couplings, while the couplings of the Z boson to fermions are a mixture of vector and axial-vector couplings. Due to the presence of both vector and axial-vector couplings, we expect to have an asymmetric distribution of the angle between the negatively-charged lepton relative to the incoming quark direction in the dilepton rest frame. Both ATLAS and CMS collaborations have measured this asymmetry using $pp \rightarrow Z/\gamma^* \rightarrow \ell^+\ell^-$ ($\ell = e, \mu$) events [7] [8]. Since the LHC is a proton-proton collider, both analyses assumed the longitudinal direction of flight of the Z boson is the same direction as that of the incoming quark. The measured asymmetry distributions are found to be consistent with theoretical predictions in the whole mass region. ATLAS also extracted $\sin^2 \theta_{eff}^\ell$ using events around the Z mass region and obtained $\sin^2 \theta_{eff}^\ell = 0.2308 \pm 0.0005$ (stat) ± 0.0006 (syst) ± 0.0009 (PDF) [7].

The current world average uncertainty on $\sin^2 \theta_{eff}^\ell$ is 17×10^{-5} and is dominated by measurements from lepton colliders [9]. Due to large production cross section and integrated luminosity expected at the LHC, the statistical uncertainty on $\sin^2 \theta_{eff}^\ell$ is expected to be negligible but we need to find ways to reduce the dominant PDF uncertainty. The current best hadron collider measurement comes from D0 with an uncertainty of 47×10^{-5} [10] that is comparable to each individual lepton collider measurement. D0 found that using $Z \rightarrow ee$ events in all categories (CC/CE/EE where C means electrons in the central calorimeter and E means electrons in the endcap calorimeter) have significantly reduced the $\sin^2 \theta_{eff}^\ell$ PDF uncertainty. It is important for the LHC experiments to also include leptons in the whole pseudorapidity coverage in their analyses. The targeted overall uncertainty with a total integrated luminosity of 3000 fb^{-1} at 14 TeV is 21×10^{-5} for each LHC experiment [11].

The current world average uncertainty on m_W is 200 ppm [12] and is dominated by Tevatron measurements. The current best measurement was performed by the CDF experiment where the contributions from experimental systematic, theoretical modelling, PDF and statistical uncertainties are all close to around 10 MeV [13]. The targeted LHC uncertainty with an integrated luminosity of 3000 fb^{-1} at 14 TeV is 5 MeV, which requires the PDF and theoretical modelling uncertainty to be around 3 MeV [11].

Due to large pileup expected at the LHC, the best precision on the m_W measurement might be achieved by fitting the lepton p_T distribution since it is less sensitive to detector effects. ATLAS studied both PDF and theoretical modelling uncertainties for the 7 TeV m_W measurement [14]. Four different PDF sets are investigated and the uncertainty on m_W within a given PDF set is found to be 10 – 20 MeV. In addition 10 – 50 MeV shifts are found between central values of different PDF sets. ATLAS varied the W p_T modelling parameters in PYTHIA and found the systematic uncertainty on m_W is close to 7 MeV.

There are many measurements at the LHC that can help reduce PDF uncertainties. One example is the W boson charge asymmetry measurement. CMS performed this measurement using 8 TeV data and the measured asymmetry is compared to predictions from three different PDF sets [15]. Experimental uncertainties on all lepton pseudorapidity bins are found to be smaller than PDF uncertainties. CMS included this result in the PDF fit and found uncertainties on u and d valence quark PDF distributions have reduced significantly. CMS also measured the W and Z inclusive cross sections at 8 TeV [16]. Different PDF sets predict different values of production cross sections and the ratio. The measured W and Z cross sections and their ratio are found to be consistent with theoretical predictions using different PDF sets.

Both ATLAS and CMS measured the W and Z boson transverse momentum distributions [17] [18] [19]. At low boson p_T ($< \sim 30 \text{ GeV}$), the production is dominated by multiple soft gluon emission and the resummation technique is needed for theoretical predictions. While at high boson p_T ($> \sim 50 \text{ GeV}$), the production is dominated by a single hard parton emission and perturbative QCD calculation is needed. The measured differential cross sections ($d\sigma/dp_T$) are compared to NNLO calculations using FEWZ [20] and predictions from a few event generators. The conclusion is that the inclusive cross section agrees with the NNLO calculation, however some shape differences are observed between measurements and predictions. These measurements will help us gain a better understanding of the W/Z boson production mechanism and further reduce the uncertainty on the m_W measurement.

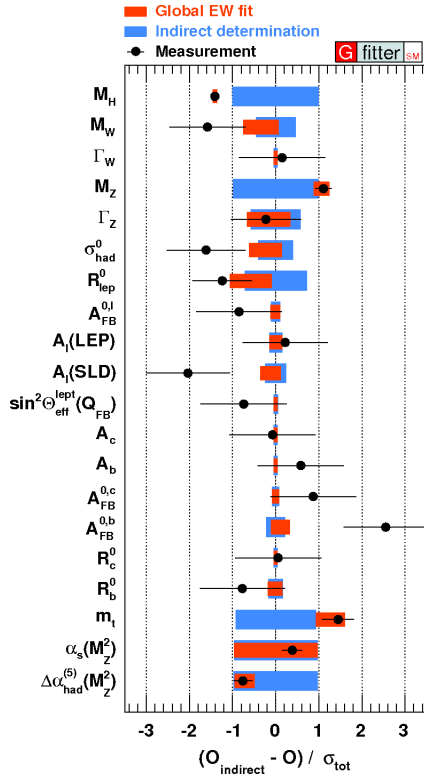


Figure 1: Comparing fit results (orange bars) with indirect determinations (blue bars) and direct measurements (data points): pull values for the SM fit defined as deviations to the indirect determinations from the Gfitter Collaboration.

4 Processes with Triple Gauge Couplings

TGC studies can be performed either using diboson processes or using mono-boson production via vector boson scattering (VBS). $ZZ\gamma$, $Z\gamma\gamma$ and $\gamma\gamma\gamma$ are forbidden. Studies of TGC processes provide fundamental tests of the electroweak sector. New physics beyond the SM could introduce anomalous TGCs that can be measured experimentally. A model-independent effective Lagrangian approach is often used to study these aTGC parameters.

Both ATLAS and CMS measured the $pp \rightarrow W^+W^- \rightarrow \ell\nu\ell'\nu'$ cross section using 7 TeV and partial 8 TeV data [21] [22] [23]. The measured fiducial cross sections are found to be 10 – 20% higher than the corresponding QCD NLO predictions. The question is whether this is due to missing higher-order corrections in theoretical predictions, upward fluctuations in data, or effects of new physics. Theorists recently performed QCD NNLO calculations and found the cross sections increased by about 8% at 7 – 8 TeV [24]. The NNLO predictions are found to be consistent with new measurements performed by both collaborations using the full 8 TeV dataset [25] [26].

Figure 2 (left) shows the comparison of the measured and predicted cross sections at 7 and 8 TeV. To reduce the SM $t\bar{t}$ background, ATLAS vetoed events with any reconstructed jets, while CMS vetoed events with more than one reconstructed jet. In addition, CMS also vetoed events with any reconstructed b -jets. To further check the modelling of the p_T of the WW system [27], CMS measured the $WW + 1$ jet cross section with the jet p_T threshold set to 20, 25 and 30 GeV. The measured fiducial cross sections for different jet p_T thresholds are also found to be consistent with theoretical predictions [26].

$W\gamma$ and $Z\gamma$ inclusive and differential cross section measurements performed by both collaborations using 7 TeV data [28] [29] indicate that QCD NLO calculations are not accurate enough since worse data-theory agreement happened for events with high p_T photons or large jet multiplicity. Theorists recently performed QCD NNLO calculations for these two processes [30]. Better agreement is observed between predicted and measured cross sections for previous measurements and new CMS $Z\gamma$ measurement using the full 8 TeV dataset [31].

ATLAS studied four lepton production in a mass range from 80 to 1000 GeV at 8 TeV [32]. For $m_{4\ell}$ close to 90 GeV, it is mainly due to $q\bar{q} \rightarrow Z \rightarrow \ell\ell Z^{(*)} \rightarrow 4\ell$; for $m_{4\ell}$ around 125 GeV, it is mainly due to Higgs production through gluon-fusion $gg \rightarrow H \rightarrow ZZ^* \rightarrow 4\ell$; while for $m_{4\ell}$ above 180 GeV, it is mainly due to t -channel production of $q\bar{q} \rightarrow Z^{(*)}Z^{(*)} \rightarrow 4\ell$, non-resonant production through quark-box diagram of $gg \rightarrow Z^{(*)}Z^{(*)} \rightarrow 4\ell$, or through s -channel production of an off-shell Higgs boson. The measured differential cross section ($d\sigma/dm_{4\ell}$) is found to be consistent with theoretical predictions with QCD NNLO and electroweak NLO calculations used for on-shell Higgs and $q\bar{q}$ production together with QCD LO calculations used for non-resonant gg -induced production. Figure 2 (right) shows the measured and predicted $m_{4\ell}$ distributions at 8 TeV. Events with $m_{4\ell} > 180$ GeV are used to extract the gg -induced signal strength with respect to the LO gg prediction. The strength is found to be 2.4 ± 1.0 (stat) ± 0.5 (syst) ± 0.8 (theory).

CMS measured the inclusive cross section for the $pp \rightarrow ZZ \rightarrow \ell\ell\nu\nu$ process [33]. This channel has a higher branching ratio compared to the $pp \rightarrow ZZ \rightarrow 4\ell$ channel but expects to have larger SM $Z(\rightarrow \ell\ell) + \text{jets}$ backgrounds. CMS chose to cut on the reduced MET and MET balance variables. The MET vector is decomposed to the parallel and perpendicular directions along the dilepton p_T axis. The reduced MET projection along direction i is defined as $-p_T^{\ell\ell,i} - R^i$ where $p_T^{\ell\ell}$ is the p_T of the dilepton system. The hadronic recoil vector \mathbf{R} is calculated using clustered or unclustered jets in the event and the one with a minimal absolute value of that reduced MET component is used. The MET balance is defined as $\text{MET}/p_T^{\ell\ell}$. A cut on the reduced MET > 65 GeV and $0.4 < \text{MET balance} < 1.8$ significantly reduced the $Z + \text{jets}$ background. The measured inclusive cross section is found to be consistent with the prediction at both 7 and 8 TeV.

CMS measured the electroweak production of a single W boson [34]. The final

state has one lepton, large MET, and two forward jets with large invariant mass and large pseudorapidity separation. The dominant background comes from the QCD production of $W + 2$ jets and is estimated using MC-simulated events. The scale factor applied on the MC estimation is extracted from a template fit to the lower side of the BDT distribution for events with $M_{jj} > 260$ GeV, which is dominated by QCD $W + 2$ jets production. The m_{jj} criteria is raised to 1000 GeV in the fiducial region and the signal contribution is obtained from a maximum-likelihood fit to the m_{jj} distribution. The measured cross section is found to be consistent with the prediction.

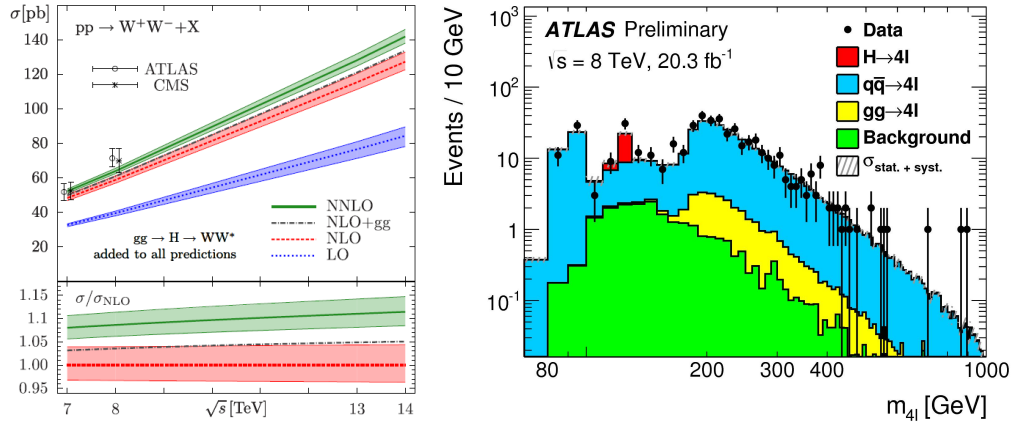


Figure 2: Left: Measured and predicted W^+W^- production cross sections at 7 and 8 TeV. Right: measured and predicted $m_{4\ell}$ distributions at 8 TeV.

5 Processes with Quartic Gauge Couplings

There are two different ways to study QGC processes: one is through the triboson production where we have three bosons in the final state, and the other is through vector boson scattering/fusion processes where each colliding quark radiates a gauge boson and these two gauge bosons interact with each other and produce two bosons and two forward jets in the final state. QGC processes are often difficult to observe due to their relatively low production cross sections. In addition, we need to remove contributions from processes involving TGC vertices, fermion-mediated or Higgs-mediated vertices that produce the same final state.

Since massless Goldstone bosons are absorbed by massless gauge bosons to become their longitudinal components, it is important to study the longitudinal scattering of two heavy gauge bosons ($V_L V_L \rightarrow V_L V_L$ with $V = W, Z$). In the SM, without Higgs-related diagrams, the cross section of VBS processes increases as a function of the

center-of-mass energy of the diboson system and violates unitarity at above ~ 1 TeV [35]. The introduction of a SM Higgs boson is the most economic way to restore the unitarity, however it is not the only way. It is possible that we have a Higgs boson with (non-)SM HVV couplings and a (or several) heavy resonance(s) that restores unitarity for the whole energy regime.

Triboson $W\gamma\gamma$ process has the largest cross section among all triboson processes. ATLAS provided the first evidence for this process using the whole data collected at 8 TeV [36]. Events are divided into inclusive ($N_{jet} \geq 0$) and exclusive ($N_{jet} = 0$) categories. The dominant background comes from processes where jets are misidentified as photons or leptons. These backgrounds are estimated from a 2-dimensional template fit to the two photon isolation energy distribution (for the jet-faked background) or the lepton isolation and MET distribution (for the lepton-faked background). The significance compared to the prediction without the $W\gamma\gamma$ process is 3σ and thus provides the first evidence for a triboson process at the LHC. Figure 3 (left) shows the measured and predicted $m_{\gamma\gamma}$ distributions.

CMS searched for the $WV\gamma$ production with $W \rightarrow \ell\nu$ and $V \rightarrow jj$ [37]. Events are selected with an isolated lepton, an isolated photon, large MET, and two jets that have an invariant mass close to the W and Z boson mass. The dominant background comes from the $W\gamma$ +jets process and its contribution is estimated using MC-simulated events. No evidence has been found for this process and upper limits on the production cross section is set.

CMS searched for $\gamma\gamma \rightarrow WW$ process using $pp \rightarrow W^+W^-p^{(*)}p^{(*)}$ events [38], where each proton radiates a photon and the final state protons have very forward pseudorapidities and are not detected. To reduce the Drell-Yan background, only the $e\mu$ final state is used. Signal events tend to have a high p_T isolated opposite-sign $e\mu$ pair with large $p_T(e\mu)$ and $m_{e\mu}$. Besides the electron and muon tracks, there are no other tracks associated with the primary collision vertex. The data is found to be 3.6σ above the background-only hypothesis. Figure 3 (right) shows the measured and predicted $p_T(e\mu)$ distributions. The dominant background for this process comes from exclusive $\gamma\gamma \rightarrow \ell^+\ell^-$ production, and ATLAS performed a measurement in both electron and muon channels at 7 TeV [39]. The measured cross sections are found to be consistent with theoretical predictions with proton absorptive effects due to the finite size of the proton taken into account.

Both ATLAS and CMS collaborations searched for the same-sign WW VBS process with two same-sign dilepton, large MET and two forward jets that has a large invariant mass and are well separated in pseudorapidity [40] [41]. ATLAS measured the cross section in an inclusive signal region and also a region dominated by electroweak production. The significance is found to be 4.5σ and 3.6σ above the background-only hypothesis for these two regions, respectively. CMS also performed a measurement of the $WZ + 2$ jets cross section.

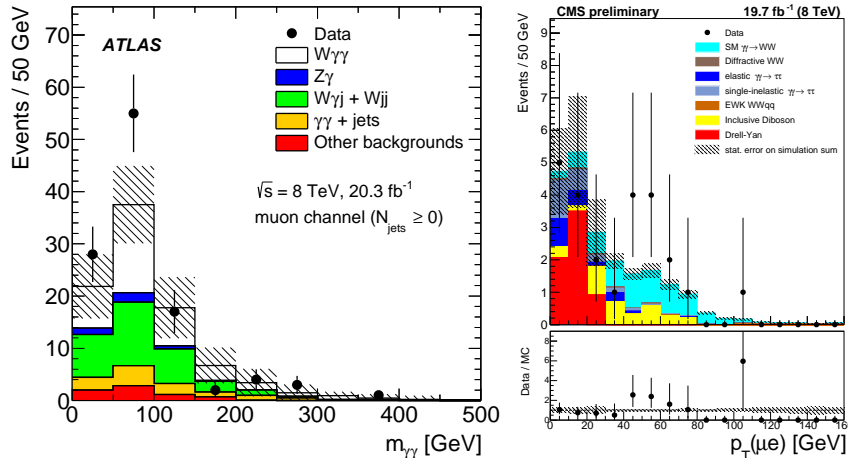


Figure 3: Left: measured and predicted $m_{\gamma\gamma}$ distributions in the ATLAS $W\gamma\gamma$ analysis. Right: measured and predicted $p_T(e\mu)$ distribution in the CMS $\gamma\gamma \rightarrow WW$ analysis.

6 Conclusions

Table 1 shows measured and predicted cross sections for TGC and QGC processes from both collaborations. Good agreement is observed for all processes.

Figure 4 (left) shows the ratio of the measured and predicted cross sections for diboson processes measured by the CMS collaboration, good agreement is observed for all processes here. The experimental uncertainties are around a few percent for most processes. Figure 4 (right) shows the measured and predicted cross sections for all SM processes performed at ATLAS. The same-sign WW VBS process has the lowest cross section that is around 1 fb.

The direct Higgs measurement at the LHC provides a critical input to the global electroweak fit. It is important to improve m_W and $\sin^2 \theta_{eff}^\ell$ measurements at the LHC to further check the SM consistency. A better understanding of PDF uncertainty is critical to reduce systematic uncertainties on these two measurements.

With large production cross sections for diboson processes, we are working toward precise measurements of diboson processes at the LHC. Experimental precisions for some processes already matched theoretical predictions. Higher-order corrections beyond the QCD NLO and electroweak LO calculations are needed for the comparison.

We started to observe processes with production cross sections close to 1 fb and provided first evidences for $W\gamma\gamma$ triboson process. In addition, we also provided first evidences for $\gamma\gamma \rightarrow W^+W^-$ and same-sign WW VBS processes. With a larger dataset expected at Run 2, we will observe more triboson and VBS processes and perform more precise measurements. It is important to check the high-mass behavior

Process (COM energy)	σ_{measured}	$\sigma_{\text{predicted}}$
ATLAS		
$pp \rightarrow W^+W^-$ (8)	$71.4 \pm 1.2(\text{stat})^{+5.0}_{-4.4}(\text{syst})^{+2.2}_{-2.1}(\text{lumi})$ pb	63.2 ± 2.0 pb
$pp \rightarrow 4\ell$ (8)	$73 \pm 4(\text{stat}) \pm 4(\text{syst}) \pm 2(\text{lumi})$ fb	65 ± 4 fb
$pp \rightarrow W\gamma\gamma$ ($N_{\text{jet}} \geq 0$) (8)	$6.1^{+1.1}_{-1.0}(\text{stat}) \pm 1.2(\text{syst}) \pm 0.2(\text{lumi})$ fb	2.90 ± 0.16 fb
$pp \rightarrow W\gamma\gamma$ ($N_{\text{jet}} > 0$) (8)	$2.9^{+0.8}_{-0.7}(\text{stat})^{+1.0}_{-0.9}(\text{syst}) \pm 0.1(\text{lumi})$ fb	1.88 ± 0.20 fb
$pp \rightarrow W^\pm W^\pm jj$ (8)	$1.3 \pm 0.4(\text{stat}) \pm 0.2(\text{syst})$ fb	0.968 ± 0.06 fb
$\gamma\gamma \rightarrow \ell^+\ell^-$ ($\ell = e$) (7)	$0.428 \pm 0.035(\text{stat}) \pm 0.018(\text{syst})$ pb	0.398 ± 0.007 pb
$\gamma\gamma \rightarrow \ell^+\ell^-$ ($\ell = \mu$) (7)	$0.628 \pm 0.032(\text{stat}) \pm 0.021(\text{syst})$ pb	0.638 ± 0.011 pb
CMS		
$pp \rightarrow W^+W^-$ (8)	$60.1 \pm 0.9(\text{stat}) \pm 4.5(\text{syst}) \pm 1.6(\text{lumi})$ pb	$59.8^{+1.3}_{-1.1}$ pb
$ZZ \rightarrow \ell\ell\nu\nu$ (7)	$67^{+20}_{-18}(\text{stat})^{+18}_{-14}(\text{syst}) \pm 2(\text{lumi})$ fb	79^{+4}_{-3} fb
$ZZ \rightarrow \ell\ell\nu\nu$ (8)	$88^{+11}_{-10}(\text{stat})^{+24}_{-18}(\text{syst}) \pm 4(\text{lumi})$ fb	97^{+4}_{-3} fb
EWK $W + 2$ jets (8)	$0.42 \pm 0.04(\text{stat}) \pm 0.09(\text{syst}) \pm 0.01(\text{lumi})$ pb	0.50 ± 0.03 pb
$pp \rightarrow p^{(*)}\mu^\pm e^\mp p^{(*)}$ (8)	$12.3^{+5.5}_{-4.4}$ fb	6.9 ± 0.6 fb
$pp \rightarrow WV\gamma$ (8)	< 311 fb	91.6 ± 21.7 fb
$pp \rightarrow W^\pm W^\pm jj$ (8)	$4.0^{+2.4}_{-2.0}(\text{stat})^{+1.1}_{-1.0}(\text{syst})$ fb	5.8 ± 1.2 fb

Table 1: Measured and predicted cross sections for TGC and QGC processes from both collaborations at different center-of-mass (COM) energies. The cross sections are different for the same process due to different phase spaces used.

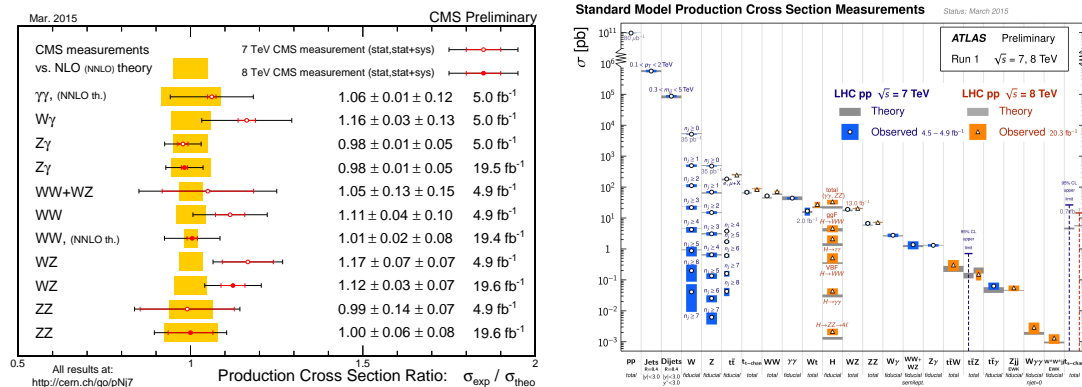
of VBS processes to gain a better understanding of the electroweak symmetry breaking mechanism.

ACKNOWLEDGMENTS

I am grateful to the DPF 2015 organization committee for inviting me to give this overview talk.

References

- [1] F. Englert and R. Brout, Phys. Rev. Lett. **13**, 321 (1964); P. Higgs, Phys. Rev. Lett. **13**, 508 (1964); G. S. Guralnik, C. R. Hagen, and T. W. B. Kibble, Phys. Rev. Lett. **13**, 585 (1964).
- [2] S.L. Glashow, Nucl. Phys. B**22** 579 (1961); A. Salam and J.C. Ward, Phys. Rev. Lett. **13** 168 (1994); S. Weinberg, Phys. Rev. Lett. **19** 1264 (1967).



- [3] M. Baak, M. Goebel, J. Haller, A. Hoecker, D. Kennedy, R. Kogler, K. Monig, M. Schott, J. Stelzer, Eur. Phys. J. **C72**, 2205 (2012).
- [4] M. Baak *et al.*, Eur. Phys. J. **C72**, 2003 (2012).
- [5] Particle Data Group Collaboration, K. Nakamura *et al.*, Review of particle physics, J. Phys. **G37** (2010) 075021.
- [6] ATLAS and CMS Collaborations, Phys. Rev. Lett. **114**, 191803 (2015).
- [7] ATLAS Collaboration, arXiv:1503.03709, accepted by JHEP.
- [8] CMS Collaboration, CMS-PAS-SMP-14-004.
- [9] G. Abbiendi *et al.* (LEP Collaborations ALEPH, DELPHI, L3 and OPAL, SLD Collaboration, LEP Electroweak Working Group, SLD Electroweak, and Heavy Flavor Groups), Phys. Rep. **427**, 257 (2006).
- [10] D0 Collaboration, Phys. Rev. Lett. **115**, 041801 (2015).
- [11] M. Baak *et al.*, arXiv:1310.6708.
- [12] CDF and D0 Collaborations, Phys. Rev. **D88**, 052018 (2013).
- [13] CDF Collaboration, Phys. Rev. Lett. **108**, 151802 (2012).
- [14] ATLAS Collaboration, ATL-PHYS-PUB-2014-015.

- [15] CMS Collaboration, CMS-PAS-SMP-14-022.
- [16] CMS Collaboration, Phys. Rev. Lett. **112**, 191802 (2014),
- [17] ATLAS Collaboration, JHEP **09** (2014) 145.
- [18] CMS Collaboration, arXiv:1504.03511, submitted to Phys. Lett. B.
- [19] CMS Collaboration, CMS-PAS-SMP-13-006.
- [20] R. Gavin, Y. Li, F. Petriello, and S. Quackenbush, Comput. Phys. Commun. **182**, 2388 (2011).
- [21] ATLAS Collaboration, Phys. Rev. D**87**, 112001 (2013).
- [22] CMS Collaboration, Eur. Phys. J. C**73** (2013) 2610.
- [23] CMS Collaboration, Phys. Lett. B**721** (2013) 190.
- [24] T. Gehrmann, M. Grazzini, S. Kallweit, P. Maierhofer, A. von Manteuffel, S. Pozzorini, D. Rathlev, and L. Tancredi, Phys. Rev. Lett. **113**, 212001 (2014).
- [25] ATLAS Collaboration, ATLAS-CONF-2014-033.
- [26] CMS Collaboration, arXiv:1507.03268, submitted to Eur. Phys. J. C.
- [27] Patrick Meade, Harikrishnan Ramani, and Mao Zeng, Phys. Rev. D**90**, 114006 (2014).
- [28] ATLAS Collaboration, Phys. Rev. D**87**, 112003 (2013).
- [29] CMS Collaboration, Phys. Rev. D **89**, 092005 (2013).
- [30] M. Grazzini, S. Kallweit, D. Rathlev, A. Torre, Phys. Lett. B**731**, 204 (2014).
- [31] CMS Collaboration, JHEP **04** (2015) 164.
- [32] ATLAS Collaboration, ATLAS-CONF-2015-031.
- [33] CMS Collaboration, arXiv:1503.05467, submitted to Eur. Phys. J. C.
- [34] CMS Collaboration, CMS-PAS-SMP-13-012.
- [35] B. W. Lee, C. Quigg, and H. B. Thacker, Phys. Rev. D**16**, 1519 (1977).
- [36] ATLAS Collaboration, Phys. Rev. Lett. **115**, 031802 (2015).
- [37] CMS Collaboration, Phys. Rev. D**90**, 032008 (2014).

- [38] CMS Collaboration, CMS-PAS-FSQ-13-008.
- [39] ATLAS Collaboration, Phys. Lett. B**749** (2015) 242.
- [40] ATLAS Collaboration, Phys. Rev. Lett. **113**, 141803 (2014).
- [41] CMS Collaboration, Phys. Rev. Lett. **114**, 051801 (2015).